

[10.1071/FP23272](https://doi.org/10.1071/FP23272)

Functional Plant Biology

Supplementary Material

Enhanced photochemical efficiency of PSII in *Prosopis juliflora* suggests contribution to invasion advantage over native C₃ xero-halophytes under salt stress

Ahmad Zia^{A,*}, Salman Gulzar^B, and Alexander V. Ruban^C

^ADepartment of Biology, University of Hafr Al-Batin, Hafr Al-Batin 31991, Saudi Arabia.

^BInstitute of Sustainable Halophyte Utilization, University of Karachi, Karachi 75270, Pakistan.

^CSchool of Biological and Behavioural Sciences, Queen Mary University of London, Mile End Road, London E1 4NS, UK.

*Correspondence to: Ahmad Zia Department of Biology, University of Hafr Al-Batin, Hafr Al-Batin 31991, Saudi Arabia Email: ahmad.zia1@outlook.com; ahmadzia@uhb.edu.sa

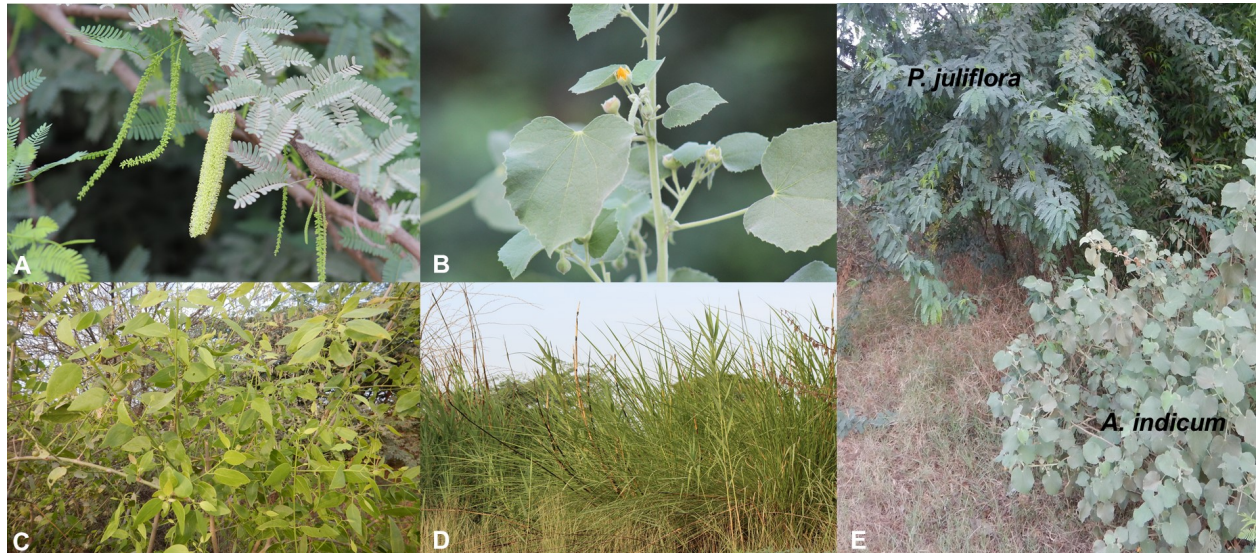


Fig. S1. Individual photographs of four xero-halophyte species: (A) *Prosopis juliflora*, (B) *Abutilon indicum*, (C) *Salvadora persica* and (D) *Phragmites karka*, along with (E) *P. juliflora* and *A. indicum* growing together under natural field conditions.

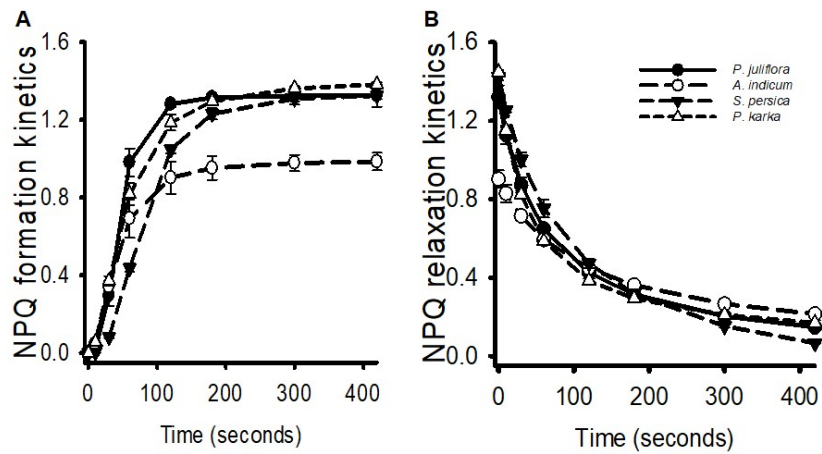


Fig. S2. Chlorophyll *a* fluorescence quenching analyses performed during the dark-to-light transition to show the kinetics of non-photochemical quenching (NPQ) in the dark-acclimated leaf samples from four xero-halophyte species: *Prosopis juliflora*, *Abutilon indicum*, *Salvadora persica*, and *Phragmites karka*, grown under natural field conditions. (a) NPQ formation kinetics during actinic light followed by (b) NPQ relaxation kinetics during the dark phase. The reported values represent the mean of individual replicates ($n = 5 \pm SE$).

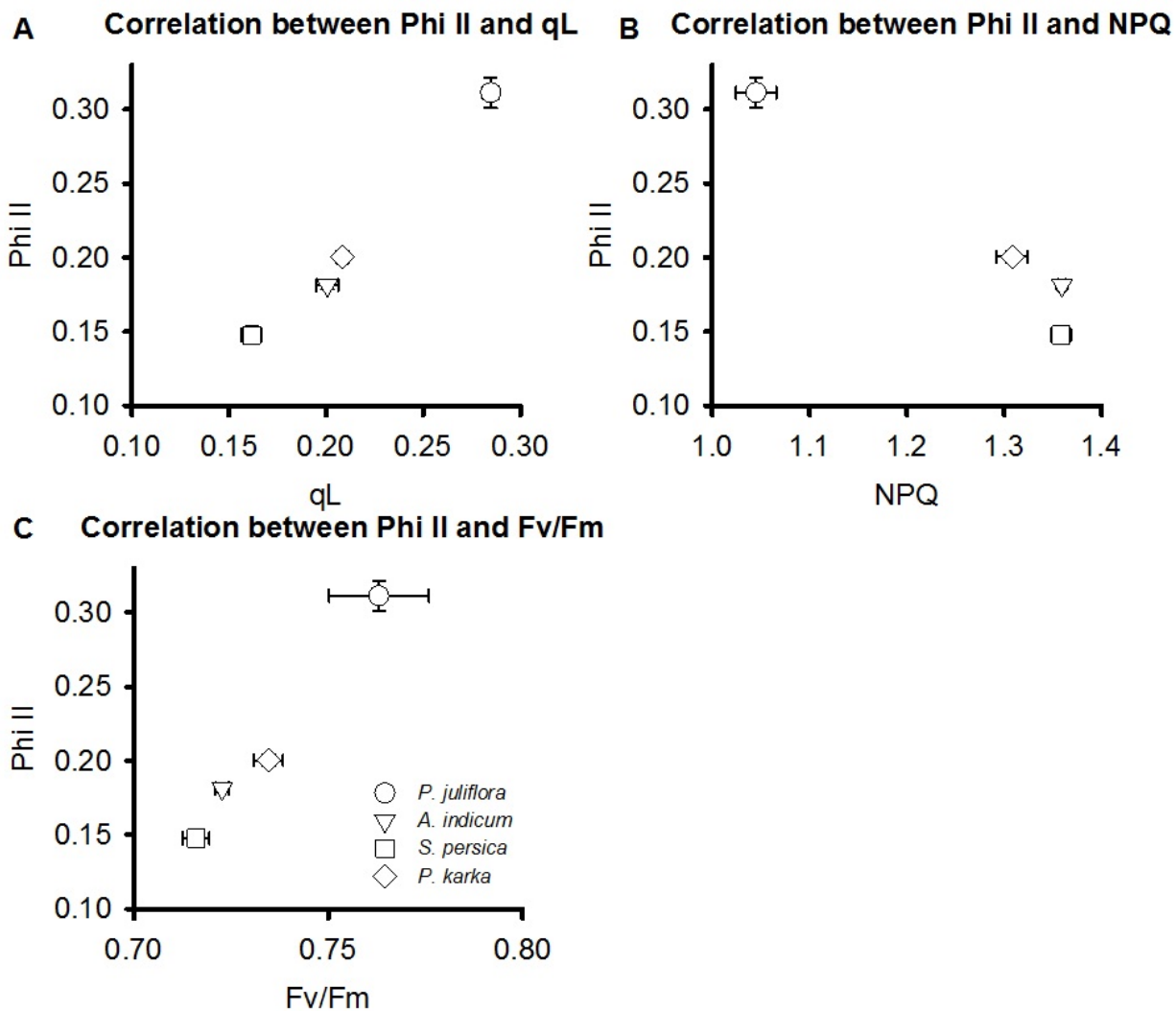


Fig. S3. Correlations between the photochemical quantum yield of PSII (ϕ_{II}) and its three determining factors of (A) fraction of open PSII RCs with oxidized Q_A primary acceptor (qL) measured as dark-to-light transition value, (B) non-photochemical quenching (NPQ) measured after the actinic light period and (C) maximum photochemical quantum efficiency of PSII (F_v/F_m) measured after dark acclimation. The parameters are from data already shown in Fig. 1 and Table 3, derived from chlorophyll *a* fluorescence quenching performed during the dark-to-light transition in dark-acclimated leaf samples from four xero-halophyte species: *Prosopis*

juliflora, *Abutilon indicum*, *Salvadora persica*, and *Phragmites karka*, grown under natural field conditions. The reported values represent the mean of individual replicates ($n = 5 \pm SE$).

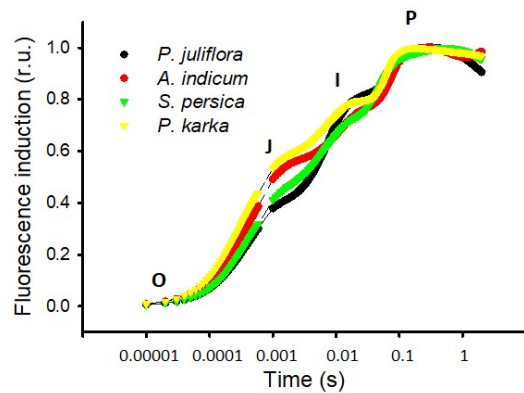


Fig. S4. Polyphasic OJIP transient rise obtained by Chlorophyll *a* fluorescence induction in dark-acclimated leaf samples from four xero-halophyte species: *Prosopis juliflora*, *Abutilon indicum*, *Salvadora persica*, and *Phragmites karka*, grown under natural field conditions. Relative variable fluorescence induction curves obtained after normalizing at O and P levels. The reported values represent the mean of individual replicates ($n = 8 \pm \text{SE}$). (Colours mentioned in the figure legend may be found in the online version of this article.)

Table S1. Technical fluorescence parameters, phenomenological and specific energy fluxes, yields of flux ratios and performance indices, as described in Table 1, measured as JIP-test parameters by fast polyphasic Chl *a* fluorescence induction in four xero-halophyte species: *Prosopis juliflora*, *Abutilon indicum*, *Salvadora persica*, and *Phragmites karka*, grown under natural field conditions. The values are mean of individual replicates ($n = 8 \pm \text{SE}$). Means with asterisks show significant difference from the species *P. juliflora* according to paired-samples *t* test ($P \leq 0.05$).

Parameter	<i>P. juliflora</i>	<i>A. indicum</i>	<i>S. persica</i>	<i>P. karka</i>
F_o	0.24 ± 0.01	$0.22^* \pm 0.01$	$0.18^* \pm 0.01$	$0.21^* \pm 0.01$
F_k	0.48 ± 0.03	0.46 ± 0.03	$0.39^* \pm 0.02$	0.48 ± 0.03
F_J	0.60 ± 0.04	0.58 ± 0.03	$0.46^* \pm 0.02$	0.61 ± 0.03
F_I	0.94 ± 0.04	$0.72^* \pm 0.03$	$0.65^* \pm 0.02$	$0.77^* \pm 0.02$
F_m	1.09 ± 0.05	$0.89^* \pm 0.02$	$0.79^* \pm 0.02$	$0.90^* \pm 0.03$
F_v	0.85 ± 0.04	$0.66^* \pm 0.02$	$0.61^* \pm 0.02$	$0.69^* \pm 0.03$
V_K	0.28 ± 0.02	$0.36^* \pm 0.04$	$0.34^* \pm 0.03$	$0.39^* \pm 0.02$
V_J	0.42 ± 0.02	$0.54^* \pm 0.05$	0.46 ± 0.04	$0.58^* \pm 0.03$
V_I	0.83 ± 0.01	$0.76^* \pm 0.02$	$0.77^* \pm 0.01$	0.81 ± 0.01
F_v/F_o	3.58 ± 0.10	$3.02^* \pm 0.18$	$3.38^* \pm 0.07$	3.32 ± 0.19
M_o	1.11 ± 0.06	$1.42^* \pm 0.11$	$1.37^* \pm 0.06$	$1.56^* \pm 0.12$
Area	304 ± 15	$246^* \pm 6$	$214^* \pm 6$	$253^* \pm 8$
ABS/CS	0.24 ± 0.01	$0.22^* \pm 0.01$	$0.18^* \pm 0.01$	$0.21^* \pm 0.01$
TR/CS	0.19 ± 0.01	$0.17^* \pm 0.01$	$0.14^* \pm 0.01$	$0.16^* \pm 0.01$
ET/CS	0.11 ± 0.01	$0.08^* \pm 0.01$	$0.08^* \pm 0.01$	$0.07^* \pm 0.01$
DI/CS	0.05 ± 0.004	$0.06^* \pm 0.006$	$0.04^* \pm 0.002$	0.05 ± 0.005
ABS/RC	3.38 ± 0.09	3.51 ± 0.17	$3.80^* \pm 0.14$	3.48 ± 0.08
TR_o/RC	2.64 ± 0.06	2.62 ± 0.09	$3.01^* \pm 0.10$	2.67 ± 0.04
ET_o/RC	1.53 ± 0.05	$1.20^* \pm 0.04$	1.44 ± 0.05	$1.11^* \pm 0.09$
DI_o/RC	0.74 ± 0.03	$0.89^* \pm 0.07$	$0.89^* \pm 0.04$	0.81 ± 0.05
ϕP_o	0.78 ± 0.002	$0.75^* \pm 0.01$	$0.77^* \pm 0.003$	0.77 ± 0.01
ϕE_o	0.45 ± 0.02	$0.35^* \pm 0.02$	0.42 ± 0.01	$0.32^* \pm 0.04$
ϕD_o	0.22 ± 0.003	$0.25^* \pm 0.01$	$0.23^* \pm 0.003$	0.23 ± 0.01

ψ_o	0.58 ± 0.03	$0.46^* \pm 0.02$	0.54 ± 0.01	$0.42^* \pm 0.04$
δR_o	0.30 ± 0.01	$0.53^* \pm 0.04$	$0.42^* \pm 0.02$	$0.48^* \pm 0.03$
$\varphi P_o / 1 - \varphi P_o$	3.58 ± 0.06	$2.98^* \pm 0.18$	$3.38^* \pm 0.07$	$3.29^* \pm 0.19$
$\psi_o / 1 - \psi_o$	1.44 ± 0.12	$0.88^* \pm 0.09$	$1.20^* \pm 0.04$	$0.75^* \pm 0.10$
PI _{ABS}	0.90 ± 0.05	$0.46^* \pm 0.02$	$0.63^* \pm 0.03$	$0.47^* \pm 0.01$
PI _{total}	4.26 ± 0.19	$6.86^* \pm 1.47$	$6.99^* \pm 0.72$	$5.14^* \pm 0.79$